

Coherent Raman imaging of live, unfixed *Schizosaccharomyces pombe* and mutants *dea2* and *pdf1*

We acquired single-cell coherent Raman microscopy data (SRS and CARS) from wild-type fission yeast and two mutants. Our aim was to collect spatially resolved biochemical data on living yeast cells. We're sharing the data and code for others to visualize and explore it!

Published Feb 4, 2026



DOI: 10.57844/arcadia-xemg-d6wv

Purpose

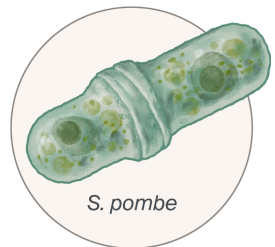
We've been using Raman spectroscopy and microscopy as label-free techniques to explore biological phenotypes. We've previously shared our work with spontaneous (incoherent) Raman systems [1] on algae [2], bacteria, archaea, and reagents [3].

Here, we sought to use coherent Raman microscopy to acquire biochemical data on living cells at subcellular resolution as part of an effort to discover measurable phenotypes in genetically defined conditions. The two techniques differ in that spontaneous (incoherent) Raman typically has high spectral throughput, whereas coherent Raman has high imaging throughput. We focused on *Schizosaccharomyces pombe* and mutants *dea2* and *pdf1* for this dataset, which is part of a larger project using yeast as models for human disease.

We're sharing the raw data, key methods, and code for image visualization and export, along with metadata. We hope this will be useful to other researchers phenotyping this species and will add to the currently limited body of coherent Raman imaging data in biology.

The approach

We chose to work with the fission yeast *Schizosaccharomyces pombe*. It's a unicellular eukaryote that's been extensively researched and has a range of available mutants. This dataset includes the *S. pombe* wild-type strain SP286 and mutant strains *_pdf1_Δ* and *_dea2_Δ* in the SP286 background. These genes are of interest to us due to their high homology to genes involved in human lysosomal storage disorders [4]. Understanding how to phenotype these strains helps us understand *S. pombe* as a model for lysosomal storage disorders.



Coherent Raman microscopy has been relatively recently explored as a useful technique for observing live biological samples without the use of stains, tags, or dyes [5]. It's been applied to study yeast cells before, and can be used to easily distinguish subcellular features such as lipid droplets [6] [7].

Strain information

Schizosaccharomyces pombe strains we used in this study were diploid and derived from the SP286 genetic background (*h⁺*/*h⁺* *ade6-M210/ade6-M216* *ura4-D18/ura4-D18* *leu1-32/leu1-32*). Gene deletion strains (*_dea2_Δ* and *_pdf1_Δ*) were generated in the SP286 background. We obtained all strains used in this study ([Table 1](#)) from [Bioneer](#).

Strain ID	Genotype	Ploidy	Selection markers	Genetic background
SP286	Wild type <i>h⁺</i> / <i>h⁺</i> <i>ade6-M210/ade6-M216</i> <i>ura4-D18/ura4-D18</i> <i>leu1-32/leu1-32</i>	Diploid	KanMX4	SP286
SPBC1198.02	<i>_dea2_Δ</i> SP286	Diploid	KanMX4	SP286
SPBC530.12c	<i>_pdf1_Δ</i> SP286	Diploid	KanMX4	SP286

Table 1. Strain information.

We acquired data on three strains of *S. pombe*.

Sample preparation

We grew three diploid *S. pombe* strains — SP286, *_pdf1_Δ*, and *_dea2_Δ* — in YES media at 30 °C and 200 rpm overnight until saturation. We pipetted 3 μ L of dense cells onto a clean glass slide, within a 4 mm wax circle. We coverslipped the slide and sealed it with VALAP (1:1 vaseline, lanolin, paraffin). We immediately imaged the cells.

Acquisition details

We used two modalities of coherent Raman imaging, stimulated Raman scattering (SRS) and coherent anti-Stokes Raman scattering (CARS). Both selectively probe individual vibrational modes and generate significantly stronger signals than spontaneous Raman, enabling rapid, label-free imaging at specific wavenumbers using two synchronized laser beams. In SRS, the Raman signal appears as a small intensity modulation of the excitation beams and scales linearly with molecular concentration, making it well suited for quantitative imaging. CARS generates a blue-shifted anti-Stokes signal that can be detected with high sensitivity, but it also includes a non-resonant background that can complicate spectral interpretation.

We acquired all data using a Leica STELLARIS CRS Coherent Raman Scattering Microscope in both SRS and epi-CARS modes. We used a 40 $×$ water immersion objective (1.1 NA) and water immersion for the condenser. Each dataset has two key fields of view, selected based on cell density and immotility.

We acquired spectra for each sample between 2,800–3,000 cm^{-1} using the “lambda scan” mode at a single z plane, using the following parameters:

- Image size: 512 \times 512
- Line scan speed: 400 Hz
- Line averaging: 2
- Pixel size: 0.11 μm
- Stokes laser wavelength: 1031.7 nm
- Stokes laser power: 0.3 W (45%)
- Pump laser step size: 0.5 nm
- Pump laser wavelength: 787.9–800.9 nm
- Pump laser power: 0.15 W (45%)

- SRS detector gain: 30%
- epiCARS detector gain: 50%

In a separate field of view, we acquired SRS and epiCARS images at eight different wavenumbers for each sample: 3,010, 2,970, 2,937, 2,850, 1,744, 1,650, 1,605, and 1,448 cm^{-1} . These wavenumbers cover a range of biologically relevant modes, summarized in [Table 2](#). We used the following acquisition parameters:

- Image size: 512×512
- Line scan speed: 200 Hz
- Line averaging: 2
- Pixel size: $0.11 \mu\text{m}$
- Stokes laser wavelength: 1031.7 nm
- Stokes laser power: 0.3 W (45%)
- Pump laser wavelength: Varies
- Pump laser power: 0.15 W (45%)
- SRS detector gain: 30%
- epiCARS detector gain: 50%

Wavenumber (cm^{-1})	Modes	Example molecules	Citation
3,010	=C-H stretch	Unsaturated fatty acids	[8]
2,970	-CH ₃ stretch	Lipid, fatty acids, nucleic acids	[6]
2,937	-CH ₃ symmetric stretch	Lipids, proteins	[6]
2,850	-CH ₂ symmetric stretch	Lipids, fatty acid chains	[8]
1,744	C=O stretch	Neutral lipids	[9]
1,650	C=O stretch (amide I)	Proteins (peptide backbone)	[10]
1,605	C=C ring stretch	Ergosterol, aromatic amino acids	[9] [11]
1,448	CH ₂ bending	Lipids, proteins, hydrocarbons	[9]

Table 2. **Key wavenumbers for this dataset.**

We acquired data for each sample at these wavenumbers, which correspond to biologically relevant bond vibrational modes.

Analysis details

We wrote code to visualize the dataset and export images and metadata. We used Python for all scripts and notebooks. We used `arcadia-pycolor` v0.6.5 to format the images generated in some of the example notebooks [12]. The images can be exported as PNG and metadata in JSON and CSV format. More details about the software, dependencies, and environment are available in the [GitHub repository](#).

AI usage

We used Claude (Sonnet 4) to help write, comment on, and review our code, then selectively incorporated its feedback. We used Claude (Opus 4.5) to review the pub and selectively incorporated its feedback. We also used Grammarly Business to suggest wording ideas and then chose which small phrases or sentence structure ideas to use.

The dataset

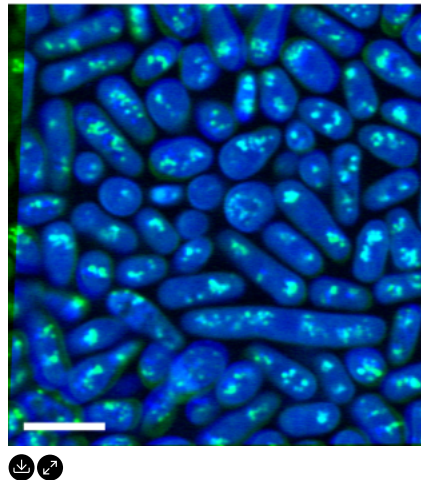


Figure 1. Representative SRS image overlay.

Composite image of two single-wavenumber SRS acquisitions, taken at $2,850$ (green) and $2,937\text{ cm}^{-1}$ (blue).

Green: Lipid droplets within cells. Blue: Entire cell biomass.

The images in the dataset contain different fields of view of the *S. pombe* cells, which appear as elongated ovals or rods. Certain subcellular structures, such as

lipid droplets, are easily visible at particular wavelengths. The single-wavenumber acquisitions can also be overlaid to produce a label-free composite that highlights various biomolecules (Figure 1).

Dataset access

Our **imaging data**, including raw LIF files and metadata files, is on [Zenodo](#).

The **code** to visualize datasets and export images and metadata is on [GitHub](#) (DOI: [10.5281/zenodo.18478294](https://doi.org/10.5281/zenodo.18478294)), including CSV and JSON [metadata](#).

Dataset limitations and caveats

As this dataset comes from living, unfixed cells in liquid culture, and the coverslips may not have perfect seals, there's movement between frames of the lambda scan and between the different single-wavenumber images. Also, while we didn't observe any noticeable damage to cells before and after laser exposure, this could have occurred. The exact wavelength we entered may differ slightly from the wavelength the laser tuned to (e.g., 2,937 vs. 2,936). Finally, the LIF files contain other acquisitions that aren't the focus of the primary dataset and visualization, and should be easily distinguishable by acquisition name. Relevant acquisitions typically follow the naming convention

“Modality_mode_wavenumber_zoom_objective_FOV.”

Next steps

We may continue to add to this dataset and the associated collection as we work with *S. pombe* and mutants. If you use this dataset, please let us know your experience — what was helpful, what information we missed, and the utility of the code repository.

Provide feedback

Social

No posts yet — mention this publication to be the first!

Contributors (A-Z)

- **Christopher Bulow**: Supervision
- **Tara Essock-Burns**: Critical feedback, Investigation
- **Ryan Lane**: Validation
- **Román Ramos Báez**: Resources
- **Sunanda Sharma**: Conceptualization, Data curation, Investigation, Methodology, Software, Writing

References

1. Braverman B, Kolb I, Mets DG, Sharma S. (2025). AutoOpenRaman: Low-cost, automated Raman spectroscopy. <https://doi.org/10.57844/arcadia-7vbd-n3ry>
2. Essock-Burns T, Kolb I, Lane R, Mets DG, Sharma S. (2025). Comparison of spontaneous Raman spectrometers. <https://doi.org/10.57844/arcadia-b670-4291>
3. Braverman B, Mets DG, Sharma S. (2025). DIY Raman spectroscopy for biological research. <https://doi.org/10.57844/arcadia-cd7e-443b>
4. Avasthi P, McGeever E, Patton AH, York R. (2024). Leveraging evolution to identify novel organismal models of human biology. <https://doi.org/10.57844/arcadia-33b4-4dc5>
5. Alfonso-García A, Mittal R, Lee ES, Potma EO. (2014). Biological imaging with coherent Raman scattering microscopy: a tutorial. <https://doi.org/10.1117/1.jbo.19.7.071407>
6. Lima C, Theron CW, Muhamadali H, Kell DB, Goodacre R. (2021). Spectral artefacts induced by moving targets in live hyperspectral stimulated Raman spectroscopy: The case of lipid droplets in yeast cells. <https://doi.org/10.1016/j.clispe.2021.100014>
7. Brackmann C, Norbeck J, Åkeson M, Bosch D, Larsson C, Gustafsson L, Enejder A. (2009). CARS microscopy of lipid stores in yeast: the impact of nutritional state and genetic background. <https://doi.org/10.1002/jrs.2356>
8. Movasaghi Z, Rehman S, Rehman IU. (2007). Raman Spectroscopy of Biological Tissues. <https://doi.org/10.1080/05704920701551530>
9. Wang K, Chen J, Martiniuk J, Ma X, Li Q, Measday V, Lu X. (2023). Species identification and strain discrimination of fermentation yeasts *Saccharomyces cerevisiae* and *Saccharomyces uvarum* using Raman spectroscopy and convolutional neural networks. <https://doi.org/10.1128/aem.01673-23>

10. Huang Y-S, Karashima T, Yamamoto M, Hamaguchi H-o. (2005). Molecular-Level Investigation of the Structure, Transformation, and Bioactivity of Single Living Fission Yeast Cells by Time- and Space-Resolved Raman Spectroscopy. <https://doi.org/10.1021/bi050179w>
11. Chiu L, Hullin Matsuda F, Kobayashi T, Torii H, Hamaguchi H. (2012). On the origin of the 1602 cm^{-1} Raman band of yeasts; contribution of ergosterol. <https://doi.org/10.1002/jbio.201200020>
12. Arcadia Science. (2024). `arcadia-pycolor` <https://github.com/arcadia-science/arcadia-pycolor>